Multidimensional Adaptive Umbrella Sampling: Applications to Main Chain and Side Chain Peptide Conformations

CHRISTIAN BARTELS,[1] MARTIN KARPLUS[2]

[1]*Laboratoire de Chimie Biophysique, Institut Le Bel, Université Louis Pasteur, 4 rue Blaise Pascal, 67000 Strasbourg, France*
[2]*Department of Chemistry, Harvard University, Cambridge, Massachusetts 02138*

Received 11 September 1996; accepted 11 February 1997

ABSTRACT: A new adaptive umbrella sampling technique for molecular dynamics simulations is described. The high efficiency of the technique renders multidimensional adaptive umbrella sampling possible and thereby enables uniform sampling of the conformational space spanned by several degrees of freedom. The efficiency is achieved by using the weighted histogram analysis method to combine the results from different simulations, by a suitable extrapolation scheme to define the umbrella potential for regions that have not been sampled, and by a criterion to identify simulations during which the system was not in equilibrium. The technique is applied to two test systems, the alanine dipeptide and the threonine dipeptide, to sample the configurational space spanned by one or two dihedral angles. The umbrella potentials applied at the end of each adaptive umbrella sampling run are equal to the negative of the corresponding potentials of mean force. The trajectories obtained in the simulations can be used to calculate dynamical variables that are of interest. An example is the distribution of the distance between the HN and the Hβ proton that can be important for the interpretation of NMR experiments. Factors influencing the accuracy of the calculated quantities are discussed. *J Comput Chem* **18**: 1450–1462, 1997

Keywords: adaptive umbrella sampling; main chain; side chain; peptide conformations

Correspondence to: M. Karplus
Contract/grant sponsor: EMBO; contract/grant number: ALTF 448-1995
Contract/grant sponsor: CNRS; contract/grant number: URA 422
Contract/grant sponsor: Association pour la Recherche contre le Cancer

CCC 0192-8651 / 97 / 121450-13

Introduction

Molecular dynamics (MD) simulations are well established as an approach that complements experimental studies of macromolecules.[1,2] Although it is possible to obtain detailed information concerning picosecond to nanosecond dynamics with current computer technology, many system properties cannot be derived from standard simulations. In general, barriers to transitions that are too high to be frequently crossed during the simulation lead to nonergodic results. For example, whereas it is possible to characterize the motions of the major conformation of an amino acid side chain for a protein of known structure, it is difficult to assess the relative populations of other conformations and to determine the effective potential (potential of mean force) for the transition from one conformer to another. A number of approaches have been developed to study such problems. They include free energy simulation methods[3] and umbrella sampling techniques.[4,5] In umbrella sampling the Hamiltonian of the system is changed by adding an ''umbrella'' potential that is chosen to direct the system into the regions of interest that are not adequately sampled in a standard simulation. After the simulations the calculated distributions are corrected for the effect of the applied umbrella potential. To define the umbrella potential one usually identifies one or a small number of degrees of freedom that contribute to the ''reaction'' coordinate most relevant for the evaluation of the desired property. Approximate uniform sampling along the reaction coordinate is achieved by applying umbrella potentials to shift the system along the coordinate in a series of simulations. An early example of the application of this method to proteins is the tyrosine ring rotation in the bovine trypsin inhibitor.[6] However, it is often difficult to define *a priori* a set of umbrella potentials for achieving the goal of uniform sampling, particularly for problems in which the reaction coordinate has to be described with more than 1 degree of freedom.[7,8] An alternative is the adaptive umbrella sampling method[7,9,10] where suitable umbrella potentials are chosen and updated in a series of simulations. In addition to its convenience and generality, the adaptive umbrella sampling technique has other advantages. Instead of restraining the system successively to different regions of space, the free energy barriers along the important degrees of freedom are reduced and the likelihood that different local minima of the system are sufficiently sampled is increased.

In the existing adaptive umbrella sampling papers[7,9,10] the general approach is similar, in principle, to the one used in this work, but there is a difference in procedure and the systems that can be treated most effectively. Paine and Scheraga[9] were interested in the prediction of native conformations of small peptides. For this purpose they derived rough estimates of the potentials of mean force for all backbone dihedral angles of the peptide and used these potentials to concentrate a further search in the low energy parts of conformational space. Hooft et al.[10] and Mezei[7] were concerned with uniform sampling along a single degree of freedom. The method presented here is applicable to uniform sampling of the conformational space spanned by several degrees of freedom. This is made possible by properly combining the results from successive simulations by using the weighted histogram analysis method (WHAM)[11–13] augmented by a new criterion to monitor the convergence. Further, the umbrella potential for regions that were not yet sampled is defined by a simple extrapolation scheme that is applicable to multidimensional umbrella potentials. Finally, a new criterion is derived to identify simulations during which the system was not in equilibrium and which should be discarded to obtain improved convergence.

The sampling of selected degrees of freedom with an iterative approach is not unique to adaptive umbrella sampling. In entropic sampling,[14–16] multicanonical simulations,[17–20] and related methods[21] the acceptance criterion in Monte Carlo simulations is changed to obtain uniform sampling of the potential energy. The same result can be achieved in MD simulations with the present technique by choosing the potential energy as the degree of freedom along which to apply the adaptive umbrella potential. This approach has been implemented and tested on peptides including an explicit solvent environment[22]; to treat such systems by a Monte Carlo method is problematic.

We describe the new adaptive umbrella sampling technique and present the details of the calculations. The technique is assessed first by calculating potentials of mean force for the $\chi 1$ dihedral angle of the threonine dipeptide, *N*-acetyl-L-threoninamide. As a 2-dimensional example and to investigate the influence of other degrees of freedom on the potential of mean force for $\chi 1$, we

determine the free energy of the threonine dipeptide as a function of the dihedrals angles $\chi 1$ and ϕ. We choose ϕ as second degree of freedom, because the probability of side chain conformations have been shown to depend on the protein backbone conformation[23,24]; we find a correlation between the $\chi 1$ and ϕ dihedral angles. It is further demonstrated how the resulting trajectories can be used to derive other quantities, for example, the expected distribution of the values of the ${}^3J_{\mathrm{H}\alpha\mathrm{H}\beta}$ coupling constant and the distribution of the distance between the HN and Hα protons. To enable comparison with existing simulation results,[25,26] we also apply the method to determine the vacuum free energy as a function of the dihedral angles ϕ and ψ for the alanine dipeptide, *N*-acetyl-L-alanine methylamide. A concluding discussion, that describes possible extensions and applications of the method is given.

Methodology

ADAPTIVE UMBRELLA SAMPLING TECHNIQUE

General Description

A series of simulations i are carried out with a potential $\mathrm{H}_i = \mathrm{H}^\circ + U_i(\lambda_1, \lambda_2, \dots)$ where the umbrella potential $U_i(\lambda_1, \lambda_2, \dots)$ is added to the Hamiltonian H° of the system and $\lambda_1, \lambda_2, \dots$ denote the degrees of freedom along which uniform sampling is desired. If $p^\circ(\lambda_1, \lambda_2, \dots)$ is the probability density for a conformation with $\lambda_1, \lambda_2, \dots$ from a simulation with H°, the corresponding probability density $p_i(\lambda_1, \lambda_2, \dots)$ for a simulation with H_i is proportional to

$$p_i(\lambda_1, \lambda_2, \dots) \propto p^\circ(\lambda_1, \lambda_2, \dots) \times \exp\left[-\frac{1}{\mathrm{RT}} U_i(\lambda_1, \lambda_2, \dots)\right]. \quad (1)$$

Uniform sampling along the degrees of freedom $\lambda_1, \lambda_2, \dots$ can be obtained, therefore, by setting

$$U(\lambda_1, \lambda_2, \dots) = \mathrm{RT} \ln p^\circ(\lambda_2, \lambda_2, \dots), \quad (2)$$

which is just the negative of the potential of mean force. Because the probability density $p^\circ(\lambda_1, \lambda_2, \dots)$ is usually not known at the beginning, an iterative procedure is used to obtain successively improved approximations, $U_i(\lambda_1, \lambda_2, \dots)$, to the ideal umbrella potential $U(\lambda_1, \lambda_2, \dots)$. The following approach is employed:

1. Initially set i to 1 and $U_1(\lambda_1, \lambda_2, \dots) = 0$.
2. Perform N_i simulation steps using H_i and collect statistics for the region in which the system is found. For this purpose the degrees of freedom $\lambda_1, \lambda_2, \dots$ are partitioned into bins with indices $k, l, \dots$ and $\lambda_1 \in (\xi_k, \xi_{k+1}]$, $\lambda_2 \in (\xi_l, \xi_{l+1}], \dots,$ where the ξ denote the boundaries between the bins and $p^\circ(\lambda_1, \lambda_2, \dots)$ is replaced by $p^\circ_{kl\dots}$. The number of times $n_{i,kl\dots}$ in which the system is found in a particular bin is determined from the simulation.
3. The statistics from all the simulations (*i.e.*, the numbers $n_{j,kl}$ with $j = 1, 2, \dots, i$) are combined to obtain an estimate $\tilde{p}^\circ_{kl\dots}$ for the probability $p^\circ_{kl\dots}$ of finding the unperturbed system in a particular bin (see below).
4. A discrete version of the umbrella potential for the next simulation, $U_{kl\dots}$, is calculated from $\tilde{p}^\circ_{kl\dots}$ using eq. (2) and a suitable extrapolation scheme for the bins $k, l, \dots$ for which no statistics were obtained (see below).
5. The continuous umbrella potential for the next simulation,

$$U_{i+1}(\lambda_1, \lambda_2, \dots, \lambda_L) = \sum_{\alpha_1} \sum_{\alpha_2} \cdots \sum_{\alpha_L} a_{\alpha_1\alpha_2\cdots\alpha_L} f^{(1)}_{\alpha_1}(\lambda_1) \times f^{(2)}_{\alpha_2}(\lambda_2) \cdots f^{(L)}_{\alpha_L}(\lambda_L), \quad (3)$$

   is represented as a linear combination of products of continuous basis functions, $\{f^{(d)}_1(\lambda_d), f^{(d)}_2(\lambda_d), \dots\}$ $(d = 1, 2, \dots, L)$ that is, trigonometric or polynomial functions of λ_d, which have to be defined by the user for each of the L degrees of freedom. The coefficients $a_{\alpha_1\alpha_2\cdots\alpha_L}$ are determined by a linear least squares fit to $U_{kl\dots}$ using singular value decomposition.[27]
6. Increment i and continue starting with step 2, or stop if the conformational space has been sampled adequately.

To simplify notation we omit indices on $U_{kl\dots}$, $\tilde{p}^\circ_{kl\dots}$ or $\bar{f}_j$ for the number of the current simulation and for the number of times eqs. (7), (8), or (10) were applied; that is, the values of these variables change after each application of eqs. (7), (8), (9), or (10).

Combination of Statistics from Different Simulations

The estimate $\tilde{p}^{\circ}_{kl\ldots}$ for the probability $p^{\circ}_{kl\ldots}$ of finding the unperturbed system in a particular bin $k, l, \ldots$ is derived from the number of times $n_{j,kl\ldots}(j = 1, 2, \ldots, i)$ in which the system was found in a particular bin during the i simulations carried out so far. According to eq. (1) the probability $p_{j,kl\ldots}$ of finding the system during simulation j in a particular bin, $kl\ldots$, can, for sufficiently small bins, be approximated by

$$p_{j,kl\ldots} = f_j c_{j,kl\ldots} p^{\circ}_{kl\ldots}$$

where

$$c_{j,kl\ldots} = \exp\left[-\frac{1}{\mathrm{RT}} U_j\left(\frac{1}{2}\{\xi_k + \xi_{k+1}\}, \frac{1}{2}\{\xi_1 + \xi_{l+1}\}, \ldots\right)\right] \quad (4)$$

and

$$f_j = \frac{1}{\sum_{kl\ldots} c_{j,kl\ldots} p^{\circ}_{kl\ldots}} \quad (5)$$

is a normalization factor to ensure $\sum_{kl\ldots} p_{j,kl\ldots} = 1$; summations are over all bins. In general, the maximum likelihood method[28,29] can be used to derive the required estimates, such as $\tilde{p}^{\circ}_{kl\ldots}$. For this purpose one has to first define the conditional probability $p(\{n_{j,kl\ldots}\} \mid \{p^{\circ}_{kl}\})$ of observing a particular set of counts $\{n_{j,kl\ldots}\}$ when the probabilities $\{p^{\circ}_{kl\ldots}\}$ are given, that is, the distribution of the $n_{j,kl\ldots}$ that one would expect in independent simulations with the Hamiltonian H_j. We assume that the $n_{j,kl\ldots}$ follow a multinomial[29] distribution, that is, that

$$p\left(\{n_{j,kl\ldots}\} \mid \{p^{\circ}_{kl}\}\right) = \frac{(\sum_{kl\ldots} g n_{j,kl\ldots})!}{\prod_{kl\ldots}(g n_{j,kl\ldots})!} \prod_{kl\ldots} p_{j,kl}^{g n_{j,kl\ldots}}. \quad (6)$$

In eq. (6) the factor $g \leq 1$ accounts for the correlation of the position of the system in subsequent time steps of a simulation, and $kl\ldots$ runs over all bins. Estimates $\tilde{p}_{kl\ldots}$ are then determined that maximize the likelihood function $L(\{p^{\circ}_{kl}\}) = \sum_j \ln(p(\{n_{j,kl\ldots}\} \mid \{p^{\circ}_{kl}\}))$ subjected to the normalization condition $\sum_{kl\ldots} p_{j,kl\ldots} = 1$ $(j = 1, 2, \ldots, i)$. Using the Lagrange multipliers α_j for the normalization conditions, this results in the following system of equations for the estimates $\tilde{p}^{\circ}_{kl\ldots}$ and $\tilde{f}_j$:

$$\forall j: \quad \sum_{kl\cdots} \tilde{p}_{j,kl\ldots} = \sum_{kl\cdots} \tilde{f}_j c_{j,kl\ldots} \tilde{p}_{kl\ldots} = 1$$

$$\forall kl\ \cdots: \quad \frac{\sum_j g n_{j,kl\ldots}}{\tilde{p}^{\circ}_{kl\ldots}} + \sum_j \alpha_j \tilde{f}_j c_{j,kl\ldots} = 0$$

$$\forall j: \quad \frac{\sum_{kl} g n_{j,kl\ldots}}{\tilde{f}_j} + \alpha_j \sum_{kl} c_{j,kl} \tilde{p}^{\circ}_{kl\ldots} = 0.$$

This can be simplified by eliminating the Lagrange multipliers α_j and using $N_j = \sum_{kl} n_{j,kl\ldots}$ to denote the number of time steps in simulation j. One obtains

$$\tilde{p}^{\circ}_{kl\ldots} = \frac{\sum_j n_{j,kl\ldots}}{\sum_j N_j \tilde{f}_j c_{j,kl\ldots}} \quad (7)$$

and

$$\tilde{f}_j = \frac{1}{\sum_{kl\ldots} c_{j,kl\ldots} \tilde{p}^{\circ}_{kl\ldots}}. \quad (8)$$

Equations (7) and (8) are commonly referred to as WHAM (Weighted Histogram Analysis Method) equations. Alternative derivations of the WHAM equations can be found in the literature.[11,12] In the same publications a convenient iterative scheme is proposed to solve this set of coupled, nonlinear equations to obtain the estimates $\tilde{p}^{\circ}_{kl\ldots}$ and $\tilde{f}_j$: starting from initial estimates for the $\tilde{f}_j$, eqs. (7) and (8) are iteratively applied until convergence is achieved. For the initial estimate we use the $\tilde{f}_j$, $j = 1, 2, \ldots, i-1$, obtained after the previous simulation $i-1$ and set $\tilde{f}_i = \tilde{f}_{i-1}$ for $i > 1$, or $\tilde{f}_i = 1$ for $i = 1$. To monitor the convergence after the application of eq. (8), we compare the deviation of the total number of counts $\sum_j n_{j,kl\ldots}$ for each bin from $\sum_j N_j \tilde{p}^{\circ}_{j,kl\ldots}$ with $\tilde{p}_{j,kl\ldots} = \tilde{f}_j c_{j,kl\ldots} \tilde{p}^{\circ}_{kl\ldots}$. For the exact solution this deviation is zero for all bins (eq. 7). We consider the result as converged if the mean square deviation for all bins is smaller than a threshold. We have set this threshold to 1. For the calculations presented in the Results section, this yields satisfactory results and eqs. (7) and (8) with the exception of the first few simulations, generally had to be applied less than 10 times to obtain converged results.

Extrapolation of Umbrella Potential

From the estimates $\tilde{p}^{\circ}_{kl\ldots}$ the umbrella potential for the next simulation

$$U_{kl\ldots} = \mathrm{RT} \ln \tilde{p}^{\circ}_{kl\ldots} \quad (9)$$

is obtained for the bins $k, l, \ldots \in S$ which were visited at least once in at least one of the simulations. For the remaining bins, $k, l, \ldots \in \bar{S}$, the umbrella potential has to be extrapolated. The resulting potential should direct the system into regions that were not sampled so far, and it should be sufficiently smooth such that no local minima are introduced. The following scheme works for multidimensional umbrella potentials applied to dihedral angle degrees of freedom: first, the umbrella potential of all bins, $k, l, \ldots \in \bar{S}$ that were not sampled is set to $U_{kl\ldots} = \min_{k'l' \in S} U_{k'l'\ldots}$, *i.e.*, to a small value that will direct the system into these regions. Setting the potential of these bins to even smaller values would increase the sampling but would also increase the danger of introducing additional local minima. In a second step the discontinuities of the potential and its derivative that were introduced in the first step are smoothed out. For this purpose each $U_{kl\ldots}(k, l, \ldots \in \bar{S})$ is replaced by

$$U'_{kl\ldots} = \frac{1}{3}(-0.3U_{k-2,l\ldots} + 1.3U_{k-1,l\ldots} + U_{k,l\ldots} + 1.3U_{k+1,l\ldots} - 0.3U_{k+2,1;\ldots}), \quad (10)$$

that is an average of the potential of the bin itself ($U_{kl\ldots}$) with a weight of 1/3, the potentials of its neighboring bins ($U_{k+1,l\ldots}$ and $U_{k-1,l\ldots}$) that each have a weight of 0.7/3, and the potentials $2U_{k-1,l;\ldots} - U_{k-2,l;\ldots}$ and $2U_{k+1,l;\ldots} - U_{k+2,l;\ldots}$ that each have a weight of 0.3/3, which are linear extrapolations for bin $k, l, \ldots$ from the potentials of the two adjacent bins, $U_{k+1,l;\ldots}$, $U_{k+2,l;\ldots}$ and $U_{k-1,l;\ldots}$, $U_{k-2,l;\ldots}$, respectively. This smoothing is done for each dimension and is repeated several times until a satisfactory potential is obtained; in practice it turned out that it is sufficient to apply the smoothing 2 times in each dimension.

Identification of Outliers in Statistics

Due to the finite number of simulations steps the number of times, $n_{j,kl\ldots}$, that the system is found in a particular bin can deviate by several magnitudes from its expected value (see a later fig. and the Results section). In particular, several local minima can exist along the degrees of freedom λ_1, $\lambda_{2,\ldots}$, of which only one or a few are sampled during the first few simulations. For the other local minima, which were not sampled, the extrapolated potential is likely to be wrong, possibly by several kilocalories per mole, relative to the actual range of barriers (0–20 kcal/mol in most cases). The way in which the possible deviations are handled has an important effect on the convergence behavior (see Results section), although less so on the final results obtained after very long simulations. It has been found that the convergence is accelerated when data that appear to involve large deviations are discarded. If prior to simulation j the system was never found in a particular bin; this bin is most likely in a region of high energy or it is separated by a barrier from the current position of the system and is not properly sampled. Assuming the latter, the results obtained for all bins $k, l, \ldots$ in simulation j with $n_{j'kl} = 0$ for $j' = 1, 2, \ldots, j$ are removed by setting $c_{j,kl\ldots} = 0$ in eqs. (7) and (8) and evaluating eqs. (7) and (9) only for bins visited at least once. Further, the results of an entire simulation j are discarded if they are significantly different from those obtained in all other simulations. For this purpose we define a measure

$$d(j) = \sum_{kl} \frac{(n_{j,kl\ldots} - m_{j,kl\ldots})^2}{m_{j,kl\ldots}} \quad (11)$$

with

$$m_{j,kl\ldots} = N_j \tilde{f}_j c_{j,kl\ldots} \tilde{p}^{\circ}_{kl\ldots} \quad (12)$$

for the deviation of the results, $n_{j,kl\ldots}$, of simulation j from the estimates of their expectation values, $m_{j,kl\ldots}$. Equation (11) is based on approximating the multinomial distribution of eq. (6) for $g = 1$ by a product of normal distributions with mean $m_{j,kl\ldots}$ and standard deviation $\sqrt{m_{j,kl\ldots}}$. If for a given simulation j, $d(j)$ is 10 times larger than the average over all other simulations, the results from this simulation are discarded.

Using this criterion assumes that exceptionally large deviations $d(j)$ are due to improper sampling of the degrees of freedom λ_1, $\lambda_{2,\ldots}$. This could cause problems in systems for which exceptionally large deviations $d(j)$ are due to rare transitions between local minima along other degrees of freedom. Application of the exclusion criterion might prevent convergence of the algorithm to the correct value in this case. In the examples studied here, only a few of the early simulations were discarded and all the simulations were kept that were acquired after every bin had been sampled at least once. Thus, the problem apparently did not arise. If outliers continue to appear during the entire simulation process, an examination could be made as to whether essential degrees of freedom are not being considered explicitly.

Calculation of Observables to Which No Umbrella Potential Was Applied

MD simulations of large systems like solvated proteins are intrinsically slow. Therefore, it is desirable that many different observables (i.e., degrees of freedom or functions of the Cartesian coordinates) can be derived from a single adaptive umbrella sampling run. Here we show that it is sufficient to collect the statistics for the degrees of freedom along which an umbrella potential is applied. Distributions of other degrees of freedom can then be obtained by weighting each of the structures in a simulation by an appropriate factor. Clearly, reliable estimates can be derived only for the observables that have been sampled sufficiently. This is the case not only for degrees of freedom along which an umbrella potential was applied, but also for degrees of freedom along which only a single relevant local minimum exists, if the simulations started from a well equilibrated structure and if they were long enough to provide reasonable sampling. In most cases, convergence of the adaptive umbrella technique requires relatively long simulations (several nanoseconds) so that the simulations are suitable to derive other quantities.

We consider the simplest case with 2 degrees of freedom k and l in which the umbrella potential depends only on k. Then one can set [eq. (4)]

$$c_{j,k} \equiv c_{j,kl} = \exp\left[-\frac{1}{\mathrm{RT}} U_j\left(\frac{1}{2}\{\xi_k + \xi_{k+1}\}\right)\right]. \quad (13)$$

The projections of $\tilde{p}^\circ_{kl}$ and $n_{j,kl}$ onto the first or second dimension are given by

$$\tilde{p}^\circ_k = \sum_l \tilde{p}^\circ_{kl}, \quad \tilde{p}^\circ_l = \sum_k \tilde{p}^\circ_{kl}, \quad n_{j,k} = \sum_l n_{j,kl}, \quad n_{j,l} = \sum_k n_{j,kl} \quad (14)$$

Equations (13) and (14) hold independent of whether or not the 2 degrees of freedom k and l are perpendicular to each other. Therefore, the following derivation is valid for all choices of the degree of freedom l, as long as the umbrella potential can be written as a function of the degree of freedom k alone. From eqs. (13) and (14) the WHAM equations, eqs. (7) and (8), can be written as

$$\tilde{p}^\circ_k = \frac{\sum_j n_{j,k}}{\sum_j N_j \tilde{f}_j c_{j,k}} \quad \text{and} \quad \tilde{f}_j = \frac{1}{\sum_k c_{j,k} \tilde{p}^\circ_k}, \quad (15)$$

that is, to obtain the probabilities of finding the system in a particular bin along the degree of freedom for which the umbrella potential is applied, it is not necessary to obtain statistics for degrees of freedom along which there is no umbrella potential.

For the other degree of freedom, again using eqs. (7), (13), and (14), we obtain

$$\tilde{p}^\circ_l = \sum_k \frac{\sum_j n_{j,kl}}{\sum_j N_j \tilde{f}_j c_{j,k}} = \sum_{jk} \alpha_k n_{j,kl} \quad \text{with} \quad \alpha_k = \frac{1}{\sum_j N_j \tilde{f}_j c_{j,k}}. \quad (16)$$

The number of counts $n_{j,kl}$ can be written as

$$n_{j,kl} = \sum_{t_j} \delta\big(K(t_j), k\big)\delta\big(L(t_j), l\big), \quad (17)$$

where the summation runs over all time steps t_j of simulation j and $K(t_j)$ and $L(t_j)$ denote the index of the bin for the first and second degree of freedom, respectively, in which the system is found in time step t_j. Using eq. (17), eq. (16) can be rewritten as

$$\begin{aligned}\tilde{p}^\circ_l &= \sum_{jk} \alpha_k \sum_{t_j} \delta\big(K(t_j), k\big)\delta\big(L(t_j), l\big) \\ &= \sum_{jt_j} \left\{\sum_k \alpha_k \delta\big(K(t_j), k\big)\right\}\delta\big(L(t_j), l\big) \\ &= \sum_{jt_j} \alpha_{K(t_j)} \delta\big(L(t_j), l\big) \end{aligned} \quad (18)$$

where $\alpha_{K(t_j)}$ is defined as in eq. (16) and the last summation runs over all steps in all of the simulations. Equation (18) shows that once statistics have been obtained for the degrees of freedom along which an umbrella potential has been applied, the distributions for other degrees of freedom (i.e., any observable that is a function of the coordinates) can be extracted by simply weighting each of the conformations with the factor $\alpha_{K(t_j)}$. Independent of the chosen degree of freedom l, the effect that the umbrella potential for k has on the sampling of l is incorporated into the factor $\alpha_{K(t_j)}$.

CALCULATION DETAILS

MD simulations were performed at 303 K using the program CHARMM[30] with the all-hydrogen parameter set PARAM22.[31,32] The time step for the integrator was set to 1 fs and the SHAKE al-

gorithm[33] was used to fix the lengths of bonds involving hydrogen atoms.

Threonine Dipeptide

For the isolated threonine dipeptide, a distance-dependent dielectric was used and all nonbonded interactions were truncated at 9 Å with a shift function.[30] The threonine dipeptide was prepared by 50 steps of steepest descent minimization, 2000 steps of dynamics at 1000 K, and cooling the system down to 303 K in a further 2000 steps of dynamics. The high temperature dynamics was needed to achieve proper equilibration. Without high temperature dynamics the threonine dipeptide had a conformation with $\phi \sim 60°$ after equilibration. Because this is one of the minima (not the global minimum that is at $\phi \sim -70°$), the structure had a tendency to remain there rather than sampling different values of ϕ when the adaptive umbrella sampling was done for $\chi 1$. This resulted in slower convergence for the adaptive umbrella sampling runs. For runs with internal coordinate constraints and thermodynamic perturbation (for which this structure would be stored as the reference, see below), it led to results that were wrong by several kilocalories per mole. Potentials of mean force for the dihedral angle $\chi 1$ were determined using adaptive umbrella sampling with the dihedral $\chi 1$ as the degree of freedom λ_1 along which umbrella potentials were applied to obtain uniform sampling. One hundred iterations ($i = 1, 2, \ldots, 100$) of the adaptive umbrella sampling algorithm were performed: each consisted of 1000 steps of equilibration and 9000 steps for the acquisition of the statistics, followed by the update of the umbrella potential. Statistics for $\chi 1$ were collected using 180 bins of 2° each. Twelve trigonometric functions, $\sin(\lambda n)$ and $\cos(\lambda n)$ ($n = 1, 2, \ldots, 6$) plus a constant were used as basis functions to represent the continuous umbrella potential [eq. (3)].

For comparison the same potential of mean force was determined with internal coordinate constraints and thermodynamic perturbation theory.[26] The system was prepared without applying any constraints by 500 steps of steepest descent minimization, 20,000 steps of dynamics at 1000 K, and cooling the system down to 303 K in a further 20,000 steps of dynamics. The resulting structure was stored as the reference structure. Starting from the reference structure, a series of simulations were performed with the dihedral angle $\chi 1$ constraint at $-180°$, $-178°$, $-176°, \ldots, +178°$. Each of these simulations consisted of 500 steps of conjugated gradient minimization, 5000 steps of MD for equilibration, and 10,000 steps of MD to calculate the free energy difference for the system in which the dihedral angle was 2° larger. The increment of 2° between subsequent $\chi 1$ angle constraints was chosen to obtain a data set that could be easily compared to the results of the adaptive umbrella sampling; meaningful results can be obtained with larger angle increments.[26]

A 2-dimensional potential of mean force of the space spanned by the $\chi 1$ and ϕ dihedral angle in the threonine dipeptide was determined using the adaptive umbrella sampling technique with the dihedrals $\chi 1$ and ϕ as the two degrees of freedom λ_1 and λ_2 along which an umbrella potential was applied. One hundred iterations were used; each consisted of 3000 steps of equilibration and 27,000 steps for the acquisition of the statistics followed by the update of the umbrella potential. To collect the statistics 36×36 bins were used with a size of $10° \times 10°$. For both dimensions, the 12 trigonometric functions, $\sin(\lambda n)$ and $\cos(\lambda n)$ ($n = 1, 2, \ldots, 6$), plus a constant were used as basis functions to represent the continuous umbrella potential [eq. (3)].

Alanine Dipeptide

For the alanine dipeptide system, two sets of calculations were done: one with a distant dependent dielectric and one with a constant dielectric ($\epsilon = 1$). All nonbonded interactions were truncated at 9 Å with a shift function.[30] In each case a 2-dimensional potential of mean force of the space spanned by the Ψ and ϕ angle was determined using the adaptive umbrella sampling technique with the dihedrals Ψ and ϕ as the 2 degrees of freedom λ_1 and λ_2. The system was prepared by 50 steps of steepest descent minimization followed by 5000 steps of dynamics at 303 K. Otherwise the same parameters were used as for the acquisition of the 2-dimensional potential of mean force of the threonine dipeptide system. The same functions were also used to represent the adaptive umbrella potential.

Results

Figure 1 shows different potentials of mean force for the dihedral angle $\chi 1$ of the threonine dipeptide. These potentials are equal to the nega-

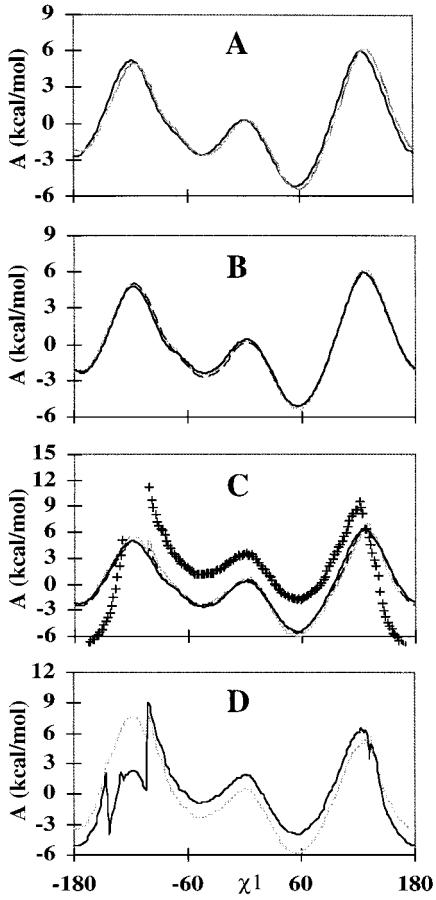

FIGURE 1. Potentials of mean force for the dihedral angle $\chi 1$ in the threonine dipeptide. (A) Comparison of the potentials obtained with different techniques: gray line, adaptive umbrella sampling technique; black line, internal coordinate constraints combined with thermodynamic perturbation. (B) Reproducibility of results from adaptive umbrella sampling. The results are shown from three runs using different random seeds for the assignment of the initial velocities. (C) Convergence of the adaptive umbrella sampling technique: (+) Result after 10 updates of the umbrella potential (100 ps of simulation time); no symbols are plotted in the region where no sampling occurred. Gray line, dashed black line, and continuous black line are the results after 20, 50, and 100 updates of the umbrella potential (200, 500, and 1000 ps of simulation time), respectively. (D) Effect of discarding the data of the fourth simulation: gray and black lines show the results after 14 updates with and without the data from the fourth simulation, respectively.

tive of the adaptive umbrella potentials from eq. (9). In Figure 1A the adaptive umbrella sampling results are validated by comparing them to the result obtained with internal coordinate constraints and thermodynamic perturbation theory. The calculated potentials are virtually indistinguishable, except that there is a slight difference for the trans rotamer ($\chi 1 = -180°$). The difference in this region might arise from the necessity of sampling local minima along degrees of freedom along which no adaptive umbrella potential is applied (see below). Figure 1B demonstrates that independent runs of the adaptive umbrella sampling technique converge to the same final potential of mean force; Figure 1C shows the convergence to the final result for a single run of the adaptive umbrella sampling technique. The crosses indicate the potential of mean force after 10 updates (100-ps simulation time) where the statistics of all 10 simulations were used. After another 10 updates the potential became virtually indistinguishable from the final result. The dramatic improvement of the latter was due partly to additional sampling and partly to the elimination of the data from the fourth simulation that violated the criterion in eq. (11). The improvement due to the elimination of the data from the fourth simulation is particularly obvious after the 14th update (Fig. 1D). Without this elimination, the potential in the region between $-180°$ and $-90°$ is distorted and comparatively low in energy. To correct this distortion, additional sampling of this region would be required. However, the umbrella potential that would be applied in subsequent simulations (derived from the negative of the potential of mean force) would be too high in this region. It would therefore direct the system away from this region, prevent additional sampling of it, and slow down the convergence of the potential. The events that led to the bad sampling in the fourth simulation are illustrated in Figure 2. In the first three simulations only the trans rotamer was sampled. The umbrella potential resulting from these three simulations had similarities to the final potential of mean force for the trans rotamer and was flat otherwise. The effective potential for the fourth simulation, $H_4 = H° + U_4(\lambda_1, \lambda_{2,\ldots})$ had three local minima at $-142°$, $-46°$ and $56°$, and an energy difference between the first and last of 9 kcal/mol. During most of the fourth simulation, the system was in the first of these minima, that is, in a location where it was unlikely to be according to the effective potential and that was separated from the rest of the conformational space by significant free energy barriers. In the last few MD steps the systems crossed the barrier at 174° and ended up in the third minimum. As a result, bins in the high energy regions of conformational space around $-142°$ were sampled much too often compared to bins in the low energy regions around 56°. For

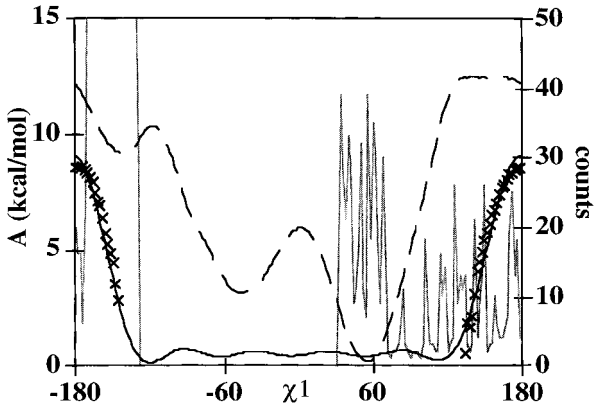

FIGURE 2. Illustration of the events leading to the bad sampling during the fourth simulation of the adaptive umbrella sampling run shown in Figure 1C, D. The x's and the black continuous line (left scale) are the umbrella potential for the fourth simulation before and after extrapolation [eq. (10)] and fitting to the set of continuous functions [eq. (3)]; long dashes (left scale) indicate the effective potential, $H_4 = H^\circ + U_4(\lambda_1, \lambda_2, \ldots)$; gray continuous lines (right scale) are the statistics, n_{4k}, of the fourth simulation. (Values larger than 50 are not shown, the highest count was 860 for the bin at $-152°$.)

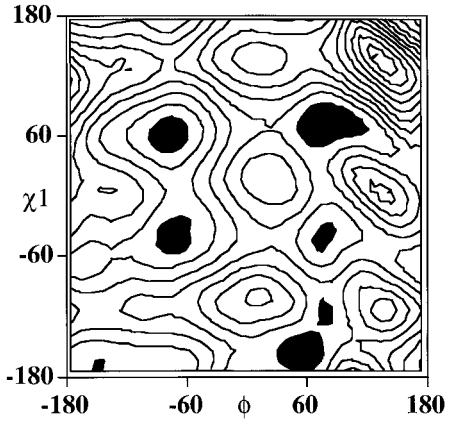

FIGURE 3. Two-dimensional potential of mean force for the two dihedral angles $\chi 1$ and ϕ in the threonine dipeptide obtained with 2-dimensional adaptive umbrella sampling. Contour lines are plotted every 2.5 kcal / mol; local minima are shown as black areas. The convergence of the calculations toward the final result was slightly slower than for the example of Figure 7; it required 43 updates of the umbrella potential until all the bins had been sampled. We note that for this simple system the potential of mean force is similar to the corresponding adiabatic potential energy map.

example, the bins at $-142°$ and at 56° were sampled 520 and 39 times, respectively, whereas according to the effective potential, the bin at 56° should have been sampled about 4,000,000 times more often than the one at $-142°$.

Further insight into the problem of obtaining correct potentials of mean force is offered by the 2-dimensional potential of mean force for the dihedrals $\chi 1$ and ϕ (Fig. 3). Note that along ϕ several local minima exist, so it is likely that the sampling of ϕ influences the outcome of the 1-dimensional potential of mean force of $\chi 1$. This conclusion is supported by Figure 4 where the data from Figure 3 is shown as 1-dimensional cross sections along $\chi 1$ at different values of ϕ and is compared to the 1-dimensional potential of mean force of $\chi 1$ obtained as the average over all the cross sections. The average 1-dimensional potential of mean force is almost identical to the final potentials of mean force obtained from 1-dimensional adaptive umbrella sampling (Fig. 1). It is also similar to the cross section at $\phi = -75°$. However, for the region between the trans ($\chi 1 = -180$) and gauche plus ($\chi 1 = -60$) rotamers, conformations exist with $\phi \sim -145°$ that are lower in energy than those with $\phi \sim -75°$. These conformations lead to a decrease of the average 1-dimensional potential by 1.9 kcal/mol relative to the potential of the cross section at $\phi = -75°$.

From these considerations it is clear that to obtain a good estimate of the potential of mean force of $\chi 1$ from 1-dimensional umbrella sampling, it is necessary that different ϕ values are sampled correctly. In particular it is indispensable to explore conformations with $\phi \sim -75°$ and $\phi \sim -145°$ (Figs. 3, 4). That this is actually the case is

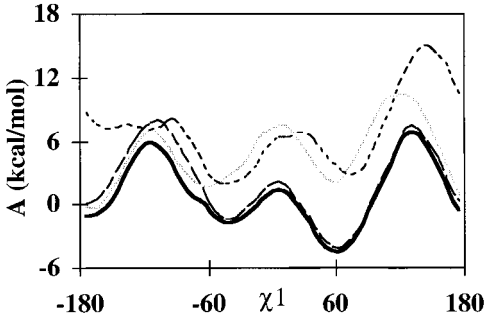

FIGURE 4. One-dimensional cross sections along $\chi 1$ through the 2-dimensional potential of mean force of Figure 3 (thin lines), and the 1-dimensional potential of mean force (thick line) for the dihedral angle $\chi 1$ obtained as the projection of the 2-dimensional potential of mean force [eq. (14)]. The gray lines are the cross section at $\phi = -145°$; the short dashes are the cross section at $\phi = 75°$; long dashes are the cross section at $\phi = -75°$.

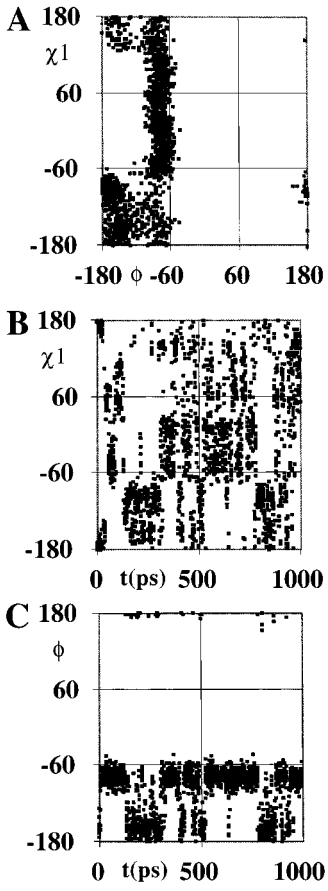

FIGURE 5. Sampling of the dihedral angles $\chi 1$ and ϕ during the 1-dimensional adaptive umbrella sampling run of Figures 1C, 1D and 2. Dihedral angles of conformations taken every 0.5 ps are shown as dots. (A) Correlation between $\chi 1$ and ϕ. (B,C) Time evolution of $\chi 1$ and ϕ, respectively.

shown in Figure 5, where the ϕ and $\chi 1$ angles are plotted that were taken from conformations sampled every 0.5 ps during the 1-dimensional adaptive umbrella sampling run of Figures 1C, 1D and 2. In some of the adaptive umbrella sampling runs, transitions did occur to the region with $\phi \sim 75°$; for example, the potential shown as a dashed line in Figure 1B is from a run in which one such transition occurred. From Figure 5 it can also be seen that the aim of the adaptive umbrella sampling is achieved; that is, there is uniform sampling of the dihedral angle $\chi 1$, and transitions between the important regions of conformational space occur fairly often.

From the trajectories, it is possible to derive properties other than the potentials of mean force. As an illustration, the expected distribution of the ${}^3J_{H\alpha H\beta}$ coupling constant and of the distance between the HN and Hβ protons is shown in Figure 6. These distributions were obtained using eq. (18) from the trajectory recorded when the potential of mean force for $\chi 1$ shown in Figure 1C was determined. Both of the distributions are dominated by conformations with $\chi 1 \sim 60°$ with small coupling constants (${}^3J_{H\alpha H\beta} \sim 2.8$ Hz) and relatively long distances (d $\sim$ 3.8 Å) between the HN and Hβ protons. A second smaller maximum corresponding to larger coupling constants (${}^3J_{H\alpha H\beta} \sim 12.8$ Hz) and smaller distances (d $\sim$ 2.9 Å) due to other conformations is present in both distributions.

Figure 7 illustrates the potentials of mean force for the conformational space spanned by the two dihedral angles ϕ and Ψ in the alanine dipeptide. The potential (Fig. 7A) obtained with the constant dielectric ($\epsilon = 1$) can be compared to the work of Tobias and Brooks.[26] Although they used a polar hydrogen model (PARAM19) and an all-hydrogen model (PARAM22) is used here, the relative free energies for four alanine dipeptide conformations given in their work are in good agreement with those obtained here (Table I). In addition to the use of different parameter sets, the differences can be attributed to the fact that with adaptive umbrella sampling an average free energy for each of the bins is determined whereas with internal coordinate constraints and thermodynamic perturbation theory one obtains free energy differences between *points* in ϕ, Ψ space. It is interesting to note that the potential obtained with the distant dependent

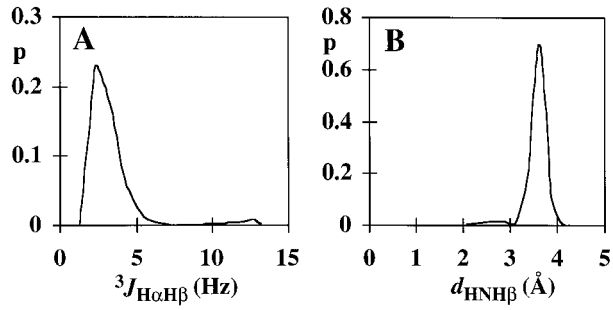

FIGURE 6. Distributions of the (A) ${}^3J_{H\alpha H\beta}$ coupling constant and (B) the distance between the HN and Hβ protons in the threonine dipeptide system when it is not perturbed by any umbrella potential. The distributions were determined from the trajectory written during an adaptive umbrella sampling run with the umbrella potential applied along the dihedral angle $\chi 1$ and eq. (18) was used to correct for the effect of the applied umbrella potentials. The coupling constants were calculated from the Karplus relation ${}^3J_{H\alpha H\beta} = 9.5\cos^2(\chi 1 - 120°) - 1.6\cos(\chi 1 - 120°) + 1.8$.

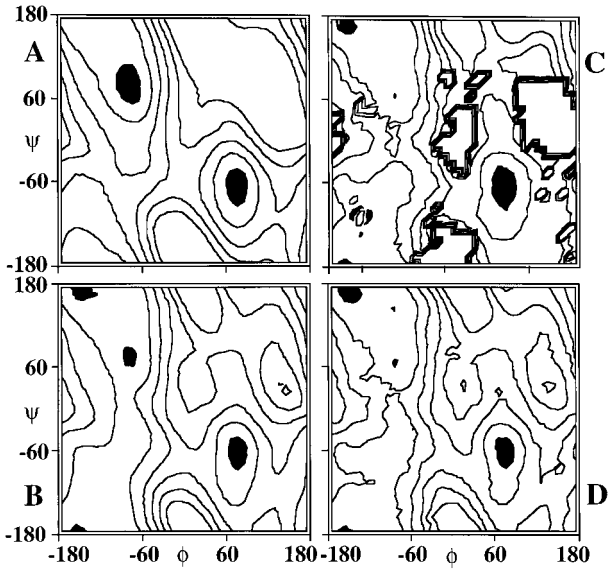

FIGURE 7. Two-dimensional potentials of mean force for the two dihedral angles ϕ and Ψ in the alanine dipeptide obtained with 2-dimensional adaptive umbrella sampling. Contour lines are plotted every 2.5 kcal / mol; local minima are shown as black areas. Shown are the results obtained with a constant dielectric after (A) 100 updates of the umbrella potential and the results obtained with distant dependent dielectric after (B) 100, (C) 10, and (D) 20 updates of the umbrella potential (corresponding to 3000, 300, and 600 ps of simulation time, respectively).

dielectric (Fig. 7B) is much more similar to the potential calculated by Anderson and Hermans[25] using explicit water than that obtained with the constant dielectric (Fig. 7A).

To demonstrate the convergence properties of the adaptive umbrella sampling technique for 2-dimensional umbrella potentials, we show results obtained after 10, 20, and 100 updates of the umbrella potential. The final potential obtained after 100 updates is shown in Figure 7B. For this result 3000 ps of MD were performed. However, after 10 updates (Fig. 6C) corresponding to only 300 ps of simulation time, the low energy parts of the potential were already similar to the final result. Only the high energy part of the potential was distorted because the corresponding parts of the conformational space (e.g., at $\phi \sim 5°$ and $\Psi \sim 5°$) were not sampled so far. After a further 10 updates (600 ps of simulation time, Fig. 7D) these distortions disappeared and the potential was virtually identical to the final result.

Discussion

The adaptive umbrella sampling technique introduced here has been shown to be an efficient molecular dynamics method for uniformly sampling the conformational space spanned by the chosen degrees of freedom. Doing a simulation for a single or a few dihedral angles with umbrella potentials assumes that either the other degrees of freedom are well sampled or that the potential of mean force of the angles of interest is independent of the other degrees of freedom. For the test systems studied here, the former is the case. To obtain first estimates for the potentials the system must diffuse through the entire conformational space spanned by the corresponding degrees of freedom. The time required depends on both the number and the nature of these degrees of freedom. In the present examples of dihedral angle potentials this was achieved in the 1-dimensional case in about 200 ps and in the 2-dimensional case in about 600 ps. This suggests that with more than 3 or 4 degrees of freedom the required simulations may be too long. The memory requirements of the technique impose corresponding limits on the size of the problem. For each bin and for each iteration two numbers ($\sigma_{j,kl\ldots}$ and $n_{j,kl\ldots}$) have to be stored.

TABLE I.
Relative Free Energies (kcal / mol) of Four Alanine Dipeptide Conformations in the Gas Phase.

Conformation	Tobias and Brooks ϕ	Tobias and Brooks Ψ	Tobias and Brooks ΔA^{a}_{vac}	Adaptive Umbrella Sampling ϕ	Adaptive Umbrella Sampling Ψ	Adaptive Umbrella Sampling ΔA^{b}_{vac}
β	−80	120	0	−80 − − 70	120 − 130	0
α_R	−80	−60	9.1	−80 − − 70	−60 − − 50	4.6
α_L	60	60	11.6	60 − 70	60 − 70	13.0
C_{7ax}	60	−80	2.4	60 − 70	−80 − − 70	1.3

[a] Determined with thermodynamic integration along paths connecting the α_R and the β conformation, the α_R and the C_{7ax} conformation, the C_{7ax} and the α_L conformation, and the β and the α_L conformation.
[b] Differences between the average free energies of conformations with ϕ and Ψ angles in the specified regions.

This is not important for 2-dimensional dihedral angle potentials for which in the present examples about 200,000 numbers had to be stored, but with current computer technology it becomes limiting for a 3- or 4-dimensional problem because it increases with the power of the number of degrees of freedom. By contrast, the CPU time needed to solve the WHAM equations does not become a problem because it depends linearly on the number of bins and the number of iterations; in the present examples it required only a few seconds to obtain converged results.

Comparing the data obtained here to other work in which potentials of mean force were obtained for small systems indicates that the performance of the adaptive umbrella sampling technique is at least comparable to the performance of conventional umbrella sampling[7, 12, 24, 25, 34–36] or that of using internal coordinate constraints and thermodynamic perturbation theory.[26] When extending such studies to larger systems (e.g., solvated proteins), the sampling of degrees of freedom along which no umbrella potential or internal coordinate constraints are applied will become limiting. It remains to be seen how the different existing methods will perform. It might well be an advantage of the adaptive umbrella sampling technique that the applied potentials smooth out free energy differences along the reaction coordinate. Thereby, free energy barriers separating different parts of the system are reduced in general and transitions between them are facilitated. By contrast, the other methods constrain the system to different positions along the reaction coordinate. This generally leads to larger free energy barriers between different parts of the system.

In the present case, the results are similar to those obtained from an adiabatic potential map. This suggests that the latter could be used in defining the initial values of the adaptive umbrella potential. However, in other cases (e.g., in the presence of solvent) very different potentials of mean force are expected.

While we were finishing this article a method similar to ours was published by Kumar et al.[37] They make use of the WHAM equations and show that their method is applicable to multidimensional umbrella potentials. An important difference is that their method is described for Monte Carlo simulations that permit use of a discontinuous umbrella potential while the present method works for MD because a continuous differentiable umbrella potential is derived. Also, they use a different extrapolation scheme, and they do not introduce means to identify outliers in the statistics that we found to be important for the convergence of the results. They report the performance of their method for the ''alanine tripeptide'' system. For a comparison with the present method, we did an adaptive umbrella sampling run to determine the free energy as a function of the ϕ and ψ angle of the central alanine residue in the blocked trialanine peptide, acetyl-Ala-Ala-Ala-methyl. We used the same parameters as for the alanine dipeptide. Detailed comparison of the performance of the two methods is difficult, because neither the system nor the computers are identical and the meaning of ''converged results'' is not well defined. Nonetheless, it seems that the present method is faster. It required only 4 h of CPU time for 100 iterations on a Silicon Graphics Indigo 2 with an R8000 2.2 processor (after 45 iterations all bins were already sampled at least once) whereas Kumar et al. report that their method required 14 h on a Silicon Graphics Indigo workstation for the calculation of a similar map. We believe that both methods are useful extensions of earlier work and will make possible interesting applications in the near future. Work is in progress on the RGDW peptide using an explicit solvent model.

Acknowledgments

We acknowledge helpful discussions with Dr. Georgios Archontis. The Institut de Développment et des Ressources en Informatique Scientifique (I.D.R.I.S.) provided an allocation of CRAY T3D computer time that was partially used for this work. C.B. was supported by the EMBO long-term fellowship ALTF 448-1995. The laboratory is partly supported by the CNRS (URA 422), the Ministère de l'Education Nationale, and a grant from the Association pour la Recherche contre le Cancer.

References

1. C. L. Brooks III, M. Karplus, and B. M. Pettitt, *Proteins: A Theoretical Perspective of Dynamics, Structure, and Thermodynamics*, Wiley, New York, 1988.
2. J. A. McCammon and S. Harvey, *Dynamics of Proteins and Nucleic Acids*, Cambridge University Press, Cambridge, U.K., 1987.
3. T. Lazaridis, C. L. Brooks III, and M. E. Paulaitis, *J. Chem. Phys.*, **95**, 7612 (1991).

4. G. M. Torrie and J. P. Valleau, *J. Comput. Phys.*, **23**, 187 (1977).
5. J. P. Valleau and G. M. Torrie, In *Statistical Mechanics, Part A: Equilibrium Techniques*, B. J. Berne, Ed., Plenum Press, New York, 1977, p. 169.
6. S. H. Northrup, M. R. Pear, C.-Y. Lee, J. A. McCammon, and M. Karplus, *Proc. Natl. Acad. Sci. USA*, **79**, 4035 (1982).
7. M. Mezei, *J. Comput. Phys.*, **68**, 237 (1987).
8. T. C. Beutler, Ph.D. thesis, ETH, Zürich, 1994.
9. G. H. Paine and H. A. Scheraga, *Biopolymers*, **24**, 1391 (1985).
10. R. W. W. Hooft, B. P. van Eijck, and J. Kroon, *J. Chem. Phys.*, **97**, 6690 (1992).
11. A. M. Ferrenberg, Ph.D. thesis, Carnegie-Mellon University, Pittsburgh, PA, 1989.
12. S. Kumar, D. Bouzida, R. H. Swendsen, P. A. Kollman, and J. M. Rosenberg, *J. Comput. Chem.*, **13**, 1011 (1992).
13. E. M. Boczko and C. L. Brooks III, *J. Phys. Chem.*, **97**, 4509 (1993).
14. J. Lee, *Phys. Rev. Lett.*, **71**, 211 (1993).
15. A. Kidera, *Proc. Natl. Acad. Sci. USA*, **92**, 9886 (1995).
16. M.-H. Hao and H. A. Scheraga, *J. Phys. Chem.*, **98**, 4940 (1994).
17. B. A. Berg, *Int. J Modern Phys.*, **C3**, 1083 (1992).
18. B. A. Berg and T. Neuhaus, *Phys. Rev. Lett.*, **68**, 9 (1992).
19. U. H. E. Hansmann and Y. Okamoto, *J. Comput. Chem.*, **14**, 1333 (1993).
20. U. H. E. Hansmann and Y. Okamoto, *Physica A*, **212**, 415 (1994).
21. A. P. Lyubartsev, A. A. Martsinovski, S. V. Shevkunov, and P. N. Vorontsov-Velyaminov, *J. Chem. Phys.*, **96**, 1776 (1992).
22. C. Bartels and M. Karplus, manuscript in preparation.
23. R. L. J. Dunbrack, Ph.D. thesis, Harvard University, Cambridge, MA, 1993.
24. R. L. J. Dunbrack and M. Karplus, *J. Mol. Biol.*, **230**, 543 (1993).
25. A. G. Anderson and J. Hermans, *Proteins Struct. Funct. Genet.*, **3**, 262 (1988).
26. D. J. Tobias and C. L. Brooks III, *J. Phys. Chem.*, **96**, 3864 (1992).
27. W. H. Press, S. A. Teukolsky, W. T. Vetterling, and B. P. Flannery, *Numerical Recipes in Fortran, The Art of Scientific Computing*, Cambridge University Press, Cambridge, U.K., 1986.
28. I. N. Bronstein and K. A. Semendjajew, *Taschenbuch der Mathematik*, Verlag Harri Deutsch, Thun, Switzerland, 1989.
29. U. Krengel, *Einführung in die Wahrscheinlichkeitstheorie und Statistik*, Vieweg, Braunschweig/Wiesbaden, Germany, 1991.
30. B. R. Brooks, R. E. Bruccoleri, B. D. Olafson, D. J. States, S. Swaminathan, and M. Karplus, *J. Comput. Chem.*, **4**, 187 (1983).
31. A. D. MacKerell, Jr. et al., *FASEB J.*, **6**, A143 (1992).
32. A. D. MacKerell, Jr. et al., manuscript in preparation.
33. J. P. Ryckaert, G. Ciccotti, and H. J. C. Berendsen, *J. Comput. Phys.*, **23**, 327 (1977).
34. T. C. Beutler and W. F. van Gunstern, *Chem. Phys. Lett.*, **237**, 308 (1995).
35. S. Kumar, J. M. Rosenberg, D. Bouzida, R. H. Swendsen, and P. A. Kollman, *J. Comput. Chem.*, **16**, 1339 (1995).
36. T. C. Beutler, T. Bremi, R. R. Ernst, and W. F. van Gunstern, *J. Phys. Chem.*, **100**, 2637 (1996).
37. S. Kumar, P. W. Payne, and M. Vásquez, *J. Comput. Chem.*, **17**, 1269 (1996).